Title

Gestational food restriction decreases placental interleukin-10 expression and markers of autophagy and endoplasmic reticulum stress in murine intrauterine growth restriction.

Permalink

https://escholarship.org/uc/item/2524m1hb

Journal

Nutrition research (New York, N.Y.), 36(10)

ISSN

0271-5317

Authors

Chu, Alison
Thamotharan, Shanthie
Ganguly, Amit
et al.

Publication Date

2016-10-01

DOI

10.1016/j.nutres.2016.08.001

Peer reviewed

Original Research

Gestational food restriction decreases placental interleukin-10 expression and markers of autophagy and endoplasmic reticulum stress in murine intrauterine growth restriction

Alison Chu[a], Shanthie Thamotharan[a], Amit Ganguly[a], Madhuri Wadehra[b], Matteo Pellegrini[c], Sherin U. Devaskar[a,*]

[a] David Geffen School of Medicine at UCLA, Department of Pediatrics, Division of Neonatology & Developmental Biology, Neonatal Research Center of the UCLA Children's Discovery and Innovation Institute, 10833 Le Conte Avenue, MDCC 22-412, Los Angeles, CA, 90095, USA
[b] David Geffen School of Medicine at UCLA, Department of Pathology, 4525 MacDonald Research Laboratories, Los Angeles, CA, 90095, USA
[c] Department of Molecular, Cell, and Developmental Biology, 3000 Terasaki Life Sciences Building, 610 Charles Young Drive East, Los Angeles, CA, 90095, USA

ABSTRACT

Intrauterine growth restriction (IUGR) affects up to 10% of pregnancies and often results in short- and long-term sequelae for offspring. The mechanisms underlying IUGR are poorly understood, but it is known that healthy placentation is essential for nutrient provision to fuel fetal growth, and is regulated by immunologic inputs. We hypothesized that in pregnancy, maternal food restriction (FR) resulting in IUGR would decrease the overall immunotolerant milieu in the placenta, leading to increased cellular stress and death. Our specific objectives were to evaluate (1) key cytokines (eg, IL-10) that regulate maternal-fetal tolerance, (2) cellular processes (autophagy and endoplasmic reticulum [ER] stress) that are immunologically mediated and important for cellular survival and functioning, and (3) the resulting IUGR phenotype and placental histopathology in this animal model. After subjecting pregnant mice to mild and moderate FR from gestational day 10 to 19, we collected placentas and embryos at gestational day 19. We examined RNA sequencing data to identify immunologic pathways affected in IUGR-associated placentas and validated messenger RNA expression changes of genes important in cellular integrity. We also evaluated histopathologic changes in vascular and trophoblastic structures as well as protein expression changes in autophagy, ER stress, and apoptosis in the mouse placentas. Several differentially expressed genes were identified in FR compared with control mice, including a considerable subset that regulates immune tolerance, inflammation, and

cellular integrity. In summary, maternal FR decreases the anti-inflammatory effect of IL-10 and suppresses placental autophagic and ER stress responses, despite evidence of dysregulated vascular and trophoblast structures leading to IUGR.

1.   Introduction

Intrauterine growth restriction (IUGR) is a poorly understood complication of pregnancy, affecting up to 10% of pregnancies. As the causes of IUGR are myriad, IUGR is thought to encompass a broad spectrum of diseases that results from poor nutrient provision to the fetus. This adverse intrauterine environment may, in some cases, result from disordered placentation or poor maternal health and nutrition [1,2]. It is critical to understand the contribution of maternal diet towards the pathophysiology of IUGR, as IUGR not only places offspring of these pregnancies at increased risk of short-term morbidity, but also at increased risk for adult-onset cardio-vascular and metabolic diseases [3-6].

The placenta plays an important role in IUGR as it is the essential organ for transportation of nutrients from maternal blood to the fetus. Studies of placental gene expression have shown that the placenta is able to sense and respond to changes in the immediate environment (eg, maternal diet) in ways that directly alter the transport of nutrients to the fetus [7-9]. The transfer of nutrients is largely mediated by blood flow and transcellular transport, via placental vasculature and across trophoblast cells. The reported placental changes seen in human IUGR include a degenerated syncytiotrophoblastic lining, fibrin deposition, hypovascular/avascular villi, and large areas of infarction [10]. These findings likely represent changes that occur in response to longstanding nutrient and oxygen insufficiency in IUGR. These changes further exacerbate poor blood flow to the fetus, resulting in poor in utero growth of the fetus.

Fig. 1. – Scheme representing crosstalk between IL-10, autophagy, ER stress, and apoptotic pathways.

The development and maintenance of placental structure and cellular function are dependent upon immune modulation with several pathways communicating to allow immune tolerance at the maternal-fetal interface. A growing body of evidence suggests that pathology in pregnancy disorders such as preeclampsia, recurrent miscarriage, and IUGR can be related to altered immune tolerance. Interleukin 10 (IL-10), an anti-inflammatory cytokine, is a key immunologic signal that is altered in these pregnancy states. It normally acts as an anti-inflammatory pleiotropic regulator in pregnancy via suppression of inflammatory cytokines, inhibition of antigen expression via major histocompatibility complex class II expression, protection against vascular dysfunction and inflammation, and modulation of endoplasmic reticulum (ER) stress and autophagy [11] (Fig. 1).

Our specific research objectives were to ascertain the effect of maternal food restriction (FR) resulting in placental insufficiency and IUGR on key cytokines in pregnancy affecting immune tolerance, for example, IL-10, and on downstream immunologic pathways regulating cellular maintenance, for example, autophagy and ER stress. As autophagy and ER stress are processes that are essential for cellular functioning in the face of pathologic stimuli such as nutrient deprivation and hypoxia, we hypothesized that maternal FR during pregnancy would result in IUGR and concomitantly decrease "anti-inflammatory" signaling in the placenta and increase cellular stress and death via alterations in autophagy and ER stress. To do this, we exposed pregnant mice to varying degrees (25% and 50% restriction of daily food intake, by weight) of maternal FR during the second half of gestation, and assessed the effect of maternal FR on placenta and embryo weight. Food restriction during gestational days (GD) 10 to 19 was chosen to mimic the chronicity of human IUGR, which more commonly manifests in the second half of pregnancy. This period was also chosen because placental function and gene expression dramatically affect fetal growth patterns during this portion of pregnancy. To initially undertake a global approach, we analyzed RNA sequencing data generated from whole placental samples to identify key genes involved in immunomodulatory pathways that were affected in our animal model of IUGR. We identified candidate genes not previously characterized in placental pathology per se, but known to be important in autophagy, ER stress, and vascular inflammation in other human diseases. We then validated altered messenger RNA expression of these specific genes by real-time polymerase chain reaction (PCR). We used a combination of Western immunoblotting as well as immunohistochemistry to evaluate whether tissue level and/or protein expression of IL-10 and markers of autophagy and ER stress pathways reflected the same directional changes as seen in the transcriptomic changes in these placentas. We also examined the placentas for histopathologic findings consistent with IUGR, and to localize associated degenerative
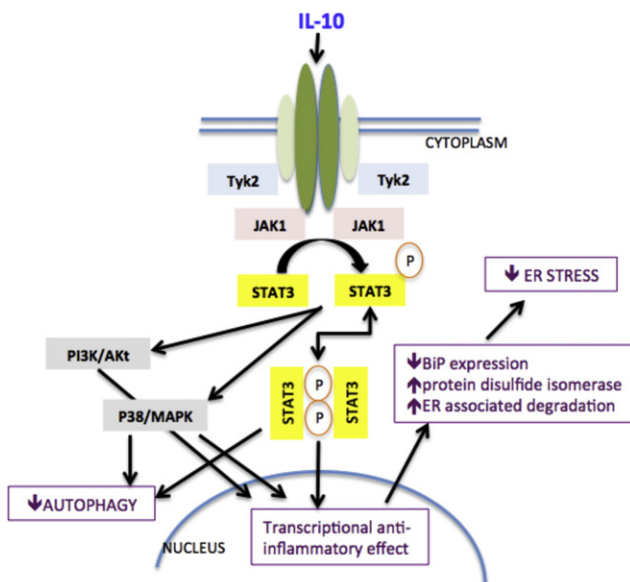
changes that we would expect to see with altered autophagy and ER stress pathways. Taken together, these experiments further our understanding of how maternal diet specifically affects the immunologic milieu at the maternal-fetal interface and the cellular health of key placental structures for nutrient provision to the fetus.

2. Methods and materials

This study was conducted in accordance with established guidelines and all protocols [12] were approved by the Animal Research Committee of the University of California Los Angeles in accordance with the guidelines set by the National Institutes of Health. C57/BL6 mice were housed in 12:12 hour light-dark cycles with ad libitum access to a standard rodent chow diet (Pico Lab Rodent Diet 20, cat# 5053, Lab Diet, St Louis, MO, USA; major ingredients included: ground corn, soybean meal, wheat middlings, whole wheat, fish meal, dried beet pulp, wheat germ, cane molasses, brewers dried yeast, ground oats, dehydrated alfalfa meal, soybean oil, whey, and calcium carbonate, and the vitamin and mineral premixes). The macronutrient content of the diet was composed of the following: carbohydrate (62.3% energy), protein (24.5% energy), and fat (13.1% energy).

2.1. Placental samples

At 8 weeks of age, male and female mice were mated overnight, and pregnant mice were identified by the presence of a vaginal plug (designated as GD 1). Pregnant females were transferred to individual cages and reared on the same chow diet ad libitum until GD 10, at which point they were randomly assigned to 3 groups (1) control group—ad libitum access to the standard rodent diet, (2) mild restriction group—restricted by 25% of their daily intake from GD 10 to 19, and (3) moderate restriction group—restricted by 50% of their daily intake from GD 10 to 19, as previously described (n = 4-5 pregnant mothers/group) [7]. On GD 19, animals were euthanized by intraperitoneal injection of 100 mg/kg of phenobarbital. The placentas were separated from the respective fetuses and collected (n = 20-25 per group). The placentas and fetuses were weighed in a Mettler AB104 precision balance (0.01 mg sensitivity), and then immediately snap-frozen and stored at –80°C until further analysis. In some cases, placentas were fixed in paraffin and then processed for immunohistochemical staining, as described below (Section 2.6).

2.2. RNA sequencing

For this analysis, only 2 groups were considered. Whole placental samples were obtained from control and 50% FR groups (n = 5/ group). Briefly, tissue from single placentas was homogenized and RNA extracted as previously described [7]. Total RNA was quantified using the Qubit RNA assay (Thermofisher Scientific, Waltham, MA, USA). Total RNA (1000 ng) was used as starting material for each sample. Library preparation was performed using the Illumina TruSeq RNA Sample Preparation kit, according to the manufacturer's instructions. Libraries were run using 50-bp single-end reads on the HiSeq2000 System (Illumina), and

reads were mapped with TopHat, which keeps unique alignments and those with up to 2 mismatches [13]. The quality of alignments was checked with FastQC and the resulting file was processed through the High Throughput Sequencing program to create a gene matrix as input for downstream analysis. Differential expressed genes sequencing [14] was used to calculate differential expression, generating reads per kilobase per million mapped reads per gene [7].

2.3. Library analysis

Genes were considered differentially expressed between control and the 50% FR group if differentially methylated regions (DMR) located close to those genes had significantly different mean expression levels as determined by Student t test, $P < .05$. Details on determination of mean methylation levels are included in Section 2.3.1 below. Pathway analysis was then conducted to identify genes that were involved in functional immunomodulatory pathways. Specifically, genes previously identified as important in inflammatory, immunologic, vascular, autophagy, or ER stress pathways in human disease were selected for further validation.

2.3.1. Statistical analysis methods used in RNA sequencing and library analysis

For each cytosine-guanine site, a t score was calculated from the t test of mean difference between the 2 groups of comparison. Sites with an absolute t score greater than or equal to 1.5 (approximately top 10%) were deemed candidate DMRs. For each candidate DMR, z score of average t score from all cytosine-guanine sites within the region was calculated. If the absolute z score was greater than threshold, as calculated based upon the false discovery rate of <5% [7], and mean methylation levels in the 2 groups differed by at least 15%, the region was considered a DMR. Genes that overlapped or had transcription start sites within 5 kbp of the DMR were considered associated genes to the DMR of interest. Genes were considered differentially expressed between the control and the 50% FR group if DMR associated with those genes had mean expression levels that were significantly different between the 2 groups, by Student t test, with unadjusted P value <.05. Log2 ratios and adjusted P values using Bonferroni correction were also calculated. False discovery rate for P value cutoffs was <5% [7].

2.4. Quantitative reverse transcriptase–polymerase chain reaction

Total cellular RNA was isolated using the RNeasy mini kit (Qiagen, Valencia, CA, USA). Complementary DNA was generated from 1 μg of total RNA from placental tissue (n = 6/group) by reverse transcription (RT) using a Superscript III Reverse Transcriptase kit (Invitrogen, San Diego, CA, USA). Amplification was performed in triplicate using Taqman-based detection on a Step One real-time quantitative PCR thermocycler (Applied Biosystems), as previously described [12]. For IL-10, the IL-10 Taqman Gene expression Assay Mm01288386_m1 was used according to the manufacturer's instructions (Applied Biosystems). For all other genes of interest, a Fam/Tamra probe was used (Eurofins, MWG Operon). Relative gene expression was calculated using the comparative C_T method [15] with

18S (Applied Biosystems, #4319413E) expression used as the internal control for normalization. The amplification cycles consisted of: 50°C for 2 minutes, 95°C for 20 seconds, then 45 cycles of 95°C for 1 second (denaturation), and 56 to 59°C for 20 seconds (annealing), followed by 72°C for 5 minutes (extension). Specific annealing temperatures, exon-spanning primers for amplification, and probe sequences for detection are provided in Table 1.

2.5. Western blotting

Bcl-2 associated X protein (BAX) and B-cell lymphoma 2 (BCL2) protein detection was undertaken to evaluate for changes in apoptosis in whole placental samples. Binding immunoglobulin protein (BIP) detection was undertaken by Western blot analysis to evaluate overall ER stress in whole placental samples. Briefly, tissue homogenates from whole placental samples were solubilized in 50 mmol/L Tris, pH 6.8, containing 2% sodium dodecyl sulfate. Protein concentration was determined by using the Bio-Rad dye-binding assay. Western blotting was performed as described previously (n = 9/group) [16]. Briefly, the solubilized protein homogenates (20 μg) were subjected to electrophoresis on 10% sodium dodecyl sulfate–polyacrylamide gels and transferred to nitrocellulose membranes (Transblot; Bio-Rad, Hercules, CA, USA). The following primary antibodies were used for signal detection: BAX antibody (Cell Signaling Technology, 1:750 dilution), BCL2 antibody (Cell Signaling Technology, 1:750 dilution), and BIP antibody (Cell Signaling Technology, 1:1000 dilution). Antivinculin antibody (Sigma-Aldrich, St Louis, MO, USA, 1:7000) was used to detect endogenous vinculin, which served as an internal control for interlane loading variability [17]. For all bands, resultant optical density was ensured as linear to the loading protein concentrations and the intensity of the protein bands was assessed by densitometry using the Scion Image software program [16].

2.6. Immunohistochemistry

Immunohistochemistry for detection of IL-10, markers of autophagy (LC3B, a ubiquitin-like protein involved in the ATG8-conjugation system, necessary for the formation of the autophagosome), vasculature (CD34+ endothelial cells), and trophoblast cells (cytokeratin staining) was performed. All tissues were rinsed in phosphate-buffered saline, fixed in cold 10% neutral buffered formalin for 24 hours, and then transferred to cold 70% ethanol. Samples were embedded in paraffin and sectioned at 5 μm thickness. A single section from each placenta was stained with hematoxylin and eosin (H&E) by the Tissue Procurement Core Laboratory at University of California, Los Angeles. Samples were deparaffinized and dehydrated in alcohol. Antigen retrieval was performed using 0.1 mol/L citrate, pH 6.0, at 95°C for 20 minutes. The slides were then incubated with antibody or control preimmune serum at the same dilution overnight. The antibody signal was visualized using the Vectastain ABC kit (Vector, PK6101; Vector Laboratories, Burlingame, CA, USA). Negative controls (no incubation with primary antibody) were included for each experiment. Anti-IL-10 (Abcam, ab33471; Abcam, Cambridge, MA, USA) was used at a dilution of 1:100; anti-CD34 (Abcam, ab81289) was used at a dilution of 1:100; pan cytokeratin (Dako, Z0622) was used at a dilution of 1:50; LC3B (Abcam, ab168831) was used at a dilution of 1:50. Antibody staining was detected using the appropriate species Vector ABC kit (Vector Laboratories, PK6106) followed by the DAB substrate [18].

Image Calibration: Staining was captured using a 4×, 10×, 20×, or 40× objective (×40, ×100, ×200, or ×400 magnification) from at least 4 nonoverlapping microscopic fields by an AxioCam CCD digital camera (Carl Zeiss). Files were saved in a 12-bit tagged image file format (.tif). To perform area analysis, unmodified, uncompressed .tif image files of staining were accessed in Photoshop as previously described [19].

2.6.1. Statistical analysis of immunohistochemistry data
We conducted quantitative analysis of vasculature using ImageJ software. The observer was blinded to the experimental groups, and using systematic random sampling, at least 3 nonoverlapping regions within the labyrinthine layer from each placental section (40× magnification images) were analyzed. Control, 25% FR, and 50% FR placentas (n = 8/group) were evaluated and standardized for equal pixel size. For vascular quantification, CD34 positively stained cells were identified and contiguous positively stained cells were marked to create an outline of the vascular area. Region of interest analysis was conducted to calculate the summative area of positively outlined areas per region.

Because of the pattern of distribution of positive staining, semiquantitative analysis of IL-10 (n = 4-7/group) and trophoblast staining (n = 8/group) was conducted by a pathologist blinded to phenotypic information. Staining was quantified by grading the overall positive staining of cells with intensities of 0

Gene	Annealing temperature	Forward primer	Reverse primer	Probe
Dram1	57°C	5′-ACACAGGAACAACTCCTCCA	5′-AACGGGAGTGCTGAAGTAGC	5′-TCTCTGCATTTCTTGGCGCAGC
Fbxo32	57°C	5′-TTCTCAGAGAGGCAGATTCG	5′-GAGAATGTGGCAGTGTTTGC	5′-CCAATCCAGCTGCCCTTTGTCA
Scd1	59°C	5′-TTCTTCTCTCACGTGGGTTG	5′-CGGGCTTGTAGTACCTCCTC	5′-CGCAAACACCCGGCTGTCAA
Pdia4	57°C	5′-GGATGCTGCTAACAACCTGA	5′-CCAGGGAGACTTTCAGGAAC	5′-CAAGTTTCACCACACTTTCAGCCCTG
Creld2	57°C	5′-TGTGTGGATGTGGATGAGTG	5′-AGCCGTTGACATTCTCACAG	5′-CATCTCCGTGCAGCGATGGC
Derl3	57°C	5′-CTCTTCGTGTTCCGCTACTG	5′-AGGAATCCCAGCAGAGTCAT	5′-AACCTCCTCCAGCATGCGG
Map3k6	56°C	5′-TACAACGCGGATGTAGTGGT	5′-AACAGAGGAGCACGTTGTTG	5′-TTCTACCACCTCGGCGTGCG
C1qa	57°C	5′-GAGCATCCAGTTTGATCGG	5′-CATCCCTGAGAGGTCTCCAT	5′-ACCACGGAGGCAGGGACACC

Table 1. – Primer and probe sequences and conditions used for qRT-PCR

to 4 akin to a Likert scale (0 = below the level of detection, 1 = weak, 2 = mild, 3 = moderate, and 4 = strong) [20].

Quantitative analysis of LC3B staining was performed by counting the number of positively- and nonstaining spongiotrophoblast cells per region of interest, located in the junctional zone. All cell counts were completed in triplicate on randomly selected fields (taken at 40×) per placental section and average cell counts calculated for each mouse placenta (n = 3-4/group).

2.7. Statistical analyses

All statistical analyses were conducted in GraphPad Prism software (version 5; GraphPad Software Inc, La Jolla, CA, USA) and data are presented as means ± SEM. Significant differences between 3 groups were analyzed using one-way analysis of variance (ANOVA) with Fisher's least significant difference, unless otherwise indicated (for quantitative RT–PCR [qRT-PCR] and Western blotting studies). Post hoc Tukey multiple comparison testing was used to determine significant differences in pairwise comparisons. When comparisons were made between 2 groups only, Student's t test was performed. All P values are reported as 2-tailed with statistical significance set at <.05 for all comparisons. Sample sizes were based upon previously published data evaluating placental gene expression using this murine model of maternal FR resulting in IUGR [7]. Power analyses conducted using gene expression data (by qRT-PCR) from that study, which showed mean relative expression = 1.0 with SD = 0.1, indicate that 5 to 8 animals per experimental group were sufficient to detect a 25% to 35% change in gene expression from the control group. These sample sizes achieve 89% power to detect a difference of at least 25% to 35% using the Hsu (with Best) multiple comparison test at a 0.05 overall significance level.

3. Results

3.1. Placenta and embryo weight

Compared with controls (n = 20), 25% FR mice (n = 25) did not demonstrate a decrease in placental weight. However, 50% FR mice (n = 21) demonstrated a significant ($P < .01$) decrease in placental weight compared with control and 25% FR mice (control, 0.08 ± 0.002 g vs 25% FR, 0.08 ± 0.002 g vs 50% FR, 0.06 ± 0.002 g). The 50% FR mice displayed a 29% decrease in placental weight compared with the control and a 31% reduction compared with the 25% FR mice. Both the 25% FR mice and 50% FR mice showed a significant ($P < .01$) decrease in embryo weight compared with controls (25% FR, 42% decrease; 50% FR, 48% decrease) (control, 1.16 ± 0.02 g vs 25% FR, 0.67 ± 0.01 g vs 50% FR, 0.61 ± 0.03 g). There was no significant difference in embryo weight between 25% and 50% FR mice.

3.2. RNA sequencing pathway analysis in placental tissue

There were almost 700 genes that were differentially expressed between 50% FR and control groups, as previously reported [7]. Approximately 15% of these genes have unknown clinical significance in human physiology or disease. Of the remainder, approximately 7% of the genes that had differential RNA expression in the 50% FR group compared with controls have been associated with immunologic function, vascular and endothelial maintenance, inflammation, autophagy, or ER stress (Table 2).

3.3. Quantitative reverse transcriptase–polymerase chain reaction

To extend the results found by RNA sequencing to the 25% FR group, we used qRT-PCR to determine gene expression in all groups, with a focus on genes involved in autophagy, ER stress, and inflammation in human disease. We validated differences in expression between control, 25% FR, and 50% FR groups (n = 6/group) for 3 genes involved in autophagy, Dram1 (control, 1.009 ± 0.059 vs 25% FR, 0.816 ± 0.094 vs 50% FR, 0.301 ± 0.062; $P < .001$), Fbxo32 (control, 1.010 ± 0.062 vs 25% FR, 0.708 ± 0.046 vs 50% FR, 0.305 ± 0.046; $P < .001$), and Scd1 (control, 1.012 ± 0.067 vs 25%FR, 0.851 ÷ 0.114 vs 50% FR, 0.581 ± 0.048; $P < .006$). Three genes which are known to be functionally important in the ER stress response, Pdia4, Creld2, and Derl3 were also significantly differentially expressed between groups (control, 1.014 ± 0.075 vs 25% FR, 0.955 ± 0.038 vs 50% FR, 0.493 ± 0.038; $P < .0001$), (control, 1.009 ± 0.057 vs 25% FR, 0.885 ± 0.054 vs 50% FR, 0.738 ± 0.089; $P < .04$), (control, 1.007 ± 0.073 vs 25% FR, 0.746 ± 0.078 vs 50% FR, 0.479 ± 0.091; $P < .001$), respectively. Lastly, 2 genes involved in vascular inflammation were found to be differentially expressed, Map3k6 (control, 1.030 ± 0.084 vs 25% FR, 1.697 ± 0.120 vs 50% FR, 2.000 ± 0.305; $P < .02$) and C1qa (control, 1.022 ± 0.088 vs 25% FR, 0.804 ± 0.096 vs 50% FR, 0.459 ± 0.059; $P < .0008$) (Fig. 2). In addition, given the key anti-inflammatory role of IL-10 in pregnancy, we quantitated its expression and found that IL-10 levels in whole placenta decreased in FR compared with control groups (control, 1.113 ± 0.214 vs 25% FR, 0.328 ± 0.058 vs 50% FR, 0.320 ± 0.072; $P < .001$).

3.4. Western immunoblotting

Our results above suggested that FR results in alterations to autophagy and ER stress pathways. To translate these differences, BAX, BCL2, and BIP protein expression were assessed by Western blot analysis. There was no significant difference in BAX ($P = .19$) or BCL2 ($P = .46$) protein expression among groups (Fig. 3A,B). However, BIP expression was down regulated in FR groups (control, 97.62 ± 5.94 vs 25% FR, 77.46 ± 4.71 vs 50% FR, 69.21 ± 4.60; $P = .0016$) (Fig. 3C). As a marker of generalized ER stress, this observation is consistent with our qRT-PCR findings of decreasing ER stress with increasing severity of FR.

3.5. Placental histopathology

Histopathology was undertaken to evaluate for differences in placental structures among groups. No appreciable differences were seen between groups in the overall architectural organization of the placenta as visualized by H&E staining (Fig. 4).

IL-10 and LC3B immunostaining was performed to evaluate for protein-level expression of inflammatory markers and

Table 2. – Genes differentially expressed between control and 50% FR groups by RNA sequencing that are involved in vascular, immunological, and inflammatory pathways.

	Gene	Average expression level (control)	Average expression level (50% FR)	Log2 fold change	P value	P value (adj)
Innate Immunity	IL-21r (interleukin 21 receptor)	1.056	0.346	−1.6	7.73E-08	.001
	IL-23r (interleukin 23 receptor)	0.366	0.078	−2.2	9.11E-06	.042
	Marco (macrophage receptor with collagenous structure)	0.019	0.856	5.5	.0002	.187
	Cebpa (CCAAT/enhancer binding protein, alpha)	6.306	9.708	0.62	.008	1
	Sfrp1 (secreted frizzled-related protein 1)	1.199	0.844	−0.5	.015	1
	Syt11 (synaptotagmin XI)	1.481	1.080	−0.45	.015	1
	Siglec1 (sialic acid binding Ig-like lectin 1, sialoadhesin)	0.660	1.132	0.78	.033	1
	Pyhin1 (pyrin and HIN domain family, member 1)	0.300	0.564	0.91	.034	1
	Isg15 (ISG15 ubiquitin-like modifier)	20.849	34.689	0.73	.045	1
Vascular and endothelial maintenance	Tnfsf15 (tumor necrosis factor superfamily, member 15)	0.072	0.019	−1.9	4.03E-05	.075
	Gm52 (syncytin a)	17.555	32.574	0.89	.0007	.339
	Wls (wntless homolog)	14.802	9.686	−0.61	.0007	.339
	Ncf1 (neutrophil cytosolic factor 1)	0.322	0.598	0.89	.001	.412
	Bmper (BMP-binding endothelial regulator)	6.383	11.646	0.87	.004	.737
	Map3k6 (mitogen activated protein kinase 6)	1.823	2.862	0.65	.006	.981
	Lyve1 (lymphatic vessel endothelial hyaluronic receptor 1)	11.950	23.472	0.97	.012	1
	Cldn5 (claudin 5)	7.497	11.338	0.60	.013	1
	Ntsr1 (neurotensin receptor 1)	0.349	0.067	−2.4	.016	1
	C5ar1 (complement component 5a receptor 1)	0.257	0.535	1.1	.021	1
	Kcnk6 (potassium inwardly-rectifying channel, K6)	3.905	2.975	−0.39	.029	1
	Lrg1 (leucine-rich alpha-2 glycoprotein 1)	2.044	3.732	0.87	.035	1
	Ucp2 (uncoupling protein 2, mitochondrial, proton carrier)	11.918	16.672	0.48	.035	1
	Trpv6 (transient receptor potential cation channel, V6)	9.530	5.234	−0.86	.049	1
	Gclm (glutamate-cysteine ligase, modifier subunit)	6.098	8.718	0.52	.049	1
Inflammation	Mmp8 (matrix metallopeptidase 8)	0.198	0.561	1.5	2.77E-05	.070
	Sfxn5 (sideroflexin 5)	0.495	0.325	−0.61	.008	1
	Slfn4 (schlafen 4)	0.433	0.736	0.77	.010	1
	IL-18rap (interleukin 18 receptor accessory protein)	0.233	0.144	−0.70	.011	1
	Tnf (tumor necrosis factor)	0.338	0.176	−0.94	.012	1
	Bok (Bcl2-related ovarian killer protein)	51.091	38.383	−0.41	.025	1
	Fpr2 (formyl peptide receptor 2)	0.149	0.354	1.25	.027	1
	Plxnc1 (plexin C1)	0.142	0.238	0.74	.032	1
	Blnk (B-cell linker)	0.485	0.742	0.61	.043	1
	C1qa (complement component 1, q subcomponent, alpha polypeptide)	5.333	10.883	1.03	.049	1
Autophagy	Fbxo32 (f box protein 32)	23.176	13.730	−0.76	.005	.808
	Scd1 (stearoyl-coenzyme A desaturase 1)	5.818	4.339	−0.42	.017	1
	Dram1 (DNA damage regulated autophagy modulator 1)	10.696	7.794	−0.46	.009	1
ER stress	Creld2 (cysteine-rich with EGF like domains 2)	42.240	27.444	−0.62	.003	.724
	Derl3 (Der1-like domain family, member 3)	23.324	14.517	−0.68	.019	1
	Pdia4 (protein disulfide isomerase associated 4)	82.834	60.377	−0.46	.010	1

Five placentas from control and 5 placentas from 50% FR mice were processed for RNA sequencing. This table represents the candidate genes identified as differentially expressed between control and 50% FR groups, by unadjusted P value < .05, involved in immunologic, inflammatory, and vascular pathways. For each gene listed, average expression level for the control and 50% FR group is reported, as well as log2 fold change, P value based upon Student t test and adjusted P value using Bonferroni correction between groups. Genes are grouped by functional roles in innate immunity, vascular and endothelial function, inflammation, autophagy, and ER stress.

bulk autophagy. Positive staining for IL-10 was seen predominantly within the junctional zone of the placenta (Fig. 5A), and overall positive staining for IL-10 was decreased with increasing degrees of FR (control, 3.60 ± 0.24 vs 25%FR, 1.75 ± 0.25 vs 50% FR, 1.25 ± 0.25; P < .0001) (Fig. 5B). Similarly, positive staining for LC3B was seen predominantly within the junctional zone and detected in mostly spongiotrophoblast cells, though occasionally seen in giant trophoblast cells (Fig. 5C). Overall numbers of spongiotrophoblasts and giant cell trophoblasts (determined by morphology) were not different between groups (P = .38 and P = .81, respectively). Average number of LC3B-positively staining spongiotrophoblast cells per section (using region of interest analysis) was significantly different between groups (control, 13.44 ± 2.39 vs 25% FR, 4.89 ± 0.29 vs 50% FR, 5.17 ± 1.18, P = .0087) (Fig. 3D).

Evaluation of vascular and trophoblast structures was specifically undertaken, as these structures are essential for nutrient provision from the mother to the fetus. Within the labyrinthine area, FR mice showed a graded decrease in vasculature with increasing severity of FR, as analyzed by CD34 immunohistochemical analysis (Fig. 6A). When summative area of vasculature per region of interest was compared, there was a significant

decrease in both FR groups compared with controls (control, 35 264 ± 3530 vs 25% FR, 23 224 ± 1623 vs 50% FR, 20 156 ± 2193; P < .01) (Fig. 6B). Overall trophoblast integrity was altered in the FR mice, as demonstrated by pan cytokeratin immunohistochemistry staining (Fig. 6C). Sections were graded 0 to 4+ on overall positivity of staining and there was a significant difference between groups (control, 3.125 ± 0.125 vs 25% FR, 2.000 ± 0.267 vs 50% FR, 1.500 ± 0.267; P < .01) (Fig. 6D). Qualitative review revealed degenerative changes of the cytokeratin-positively staining structures with a decreased percentage of positively stained cells overall in FR groups compared with control.

4. Discussion

Our animal study demonstrates that maternal nutrient deprivation during pregnancy affects the immunologic milieu in the placenta, specifically affecting both gene and protein expression of IL-10 and associated cellular stress responses to nutrient deprivation via autophagy and ER stress. Our findings are consistent with our hypothesis that IL-10
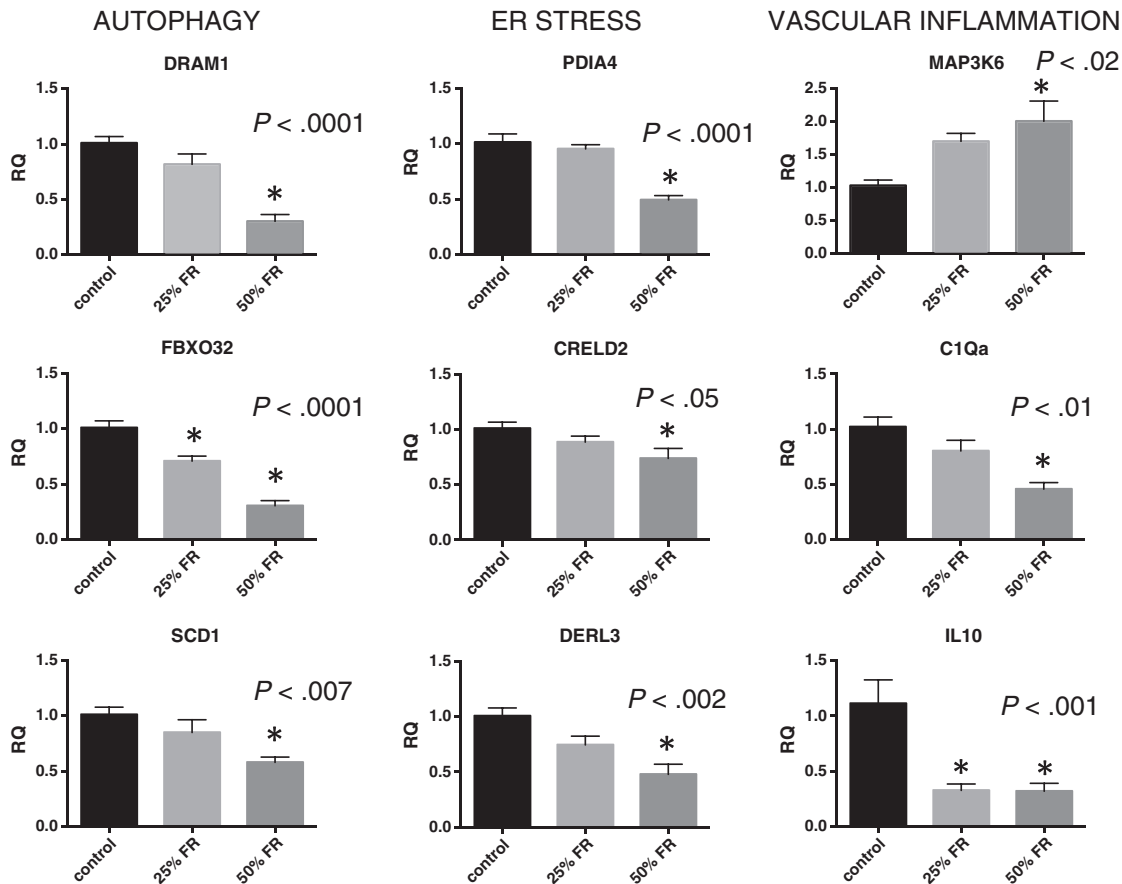

Fig. 2. – qRT-PCR validation of placental RNA expression of genes involved in vascular inflammation, autophagy, and ER stress in mice exposed to maternal FR. For each candidate gene, average mRNA expression level from control, 25% FR, and 50% FR groups (n = 6/group, based on power calculations for detecting a 25% difference in mean expression between groups to achieve 89% power at a 0.05 overall significance level) was calculated by qRT-PCR. Data are represented in graphs as means ± SEM. Asterisks indicate a significant difference between indicated FR group compared with control (P < .05) by post hoc Tukey's multiple comparison testing. Reported P value for each gene is by one-way ANOVA between all 3 groups.
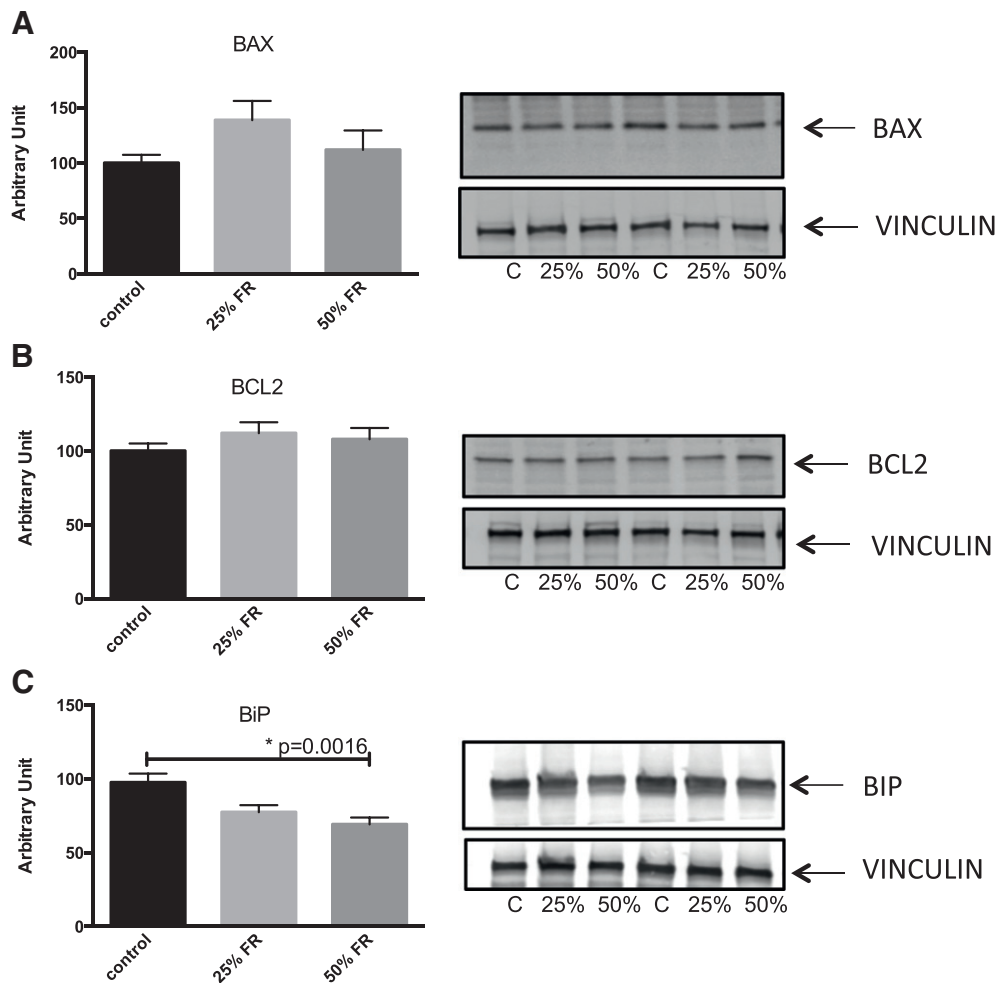
Fig. 3. – Western immunoblotting of apoptosis and ER stress markers in the placentas of gestational FR-exposed mice. Representative blots of (A) BAX, (B) BCL2 proteins as markers of apoptosis, and (C) BIP as a marker of ER stress are shown. There were no significant differences between groups for BAX and BCL2 expression. BIP expression, however, was decreased in both the 25% and 50% FR groups, compared with controls. Data are represented in graphs as means ± SEM. Asterisk indicates *P* < .05 by ANOVA. C, control; 25%, 25% FR group; 50%, 50% FR group (n = 9/group).

expression is decreased in maternal food-restricted placentas. These findings are in line with human data showing that placental insufficiency uniformly seen in various disorders of pregnancy such as recurrent miscarriages, preeclampsia, and/or IUGR may be due to disordered immune tolerance and/or dysregulation of IL-10 [11,21-23].

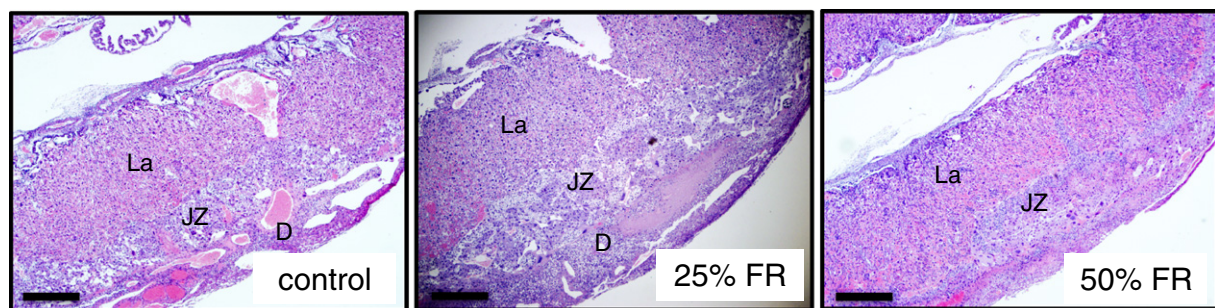IL-10 is a known key anti-inflammatory cytokine in pregnancy, but has been shown in other inflammatory

Fig. 4. – Hematoxylin and eosin staining of control, mild, and moderate FR mouse placentas at 4× magnification: representative murine placental sections stained by H&E from control, mild-, and moderate-FR exposed mice (n = 8/group). La, labyrinth; JZ, junctional zone; D, decidua. Scale bars represent 500 μm.
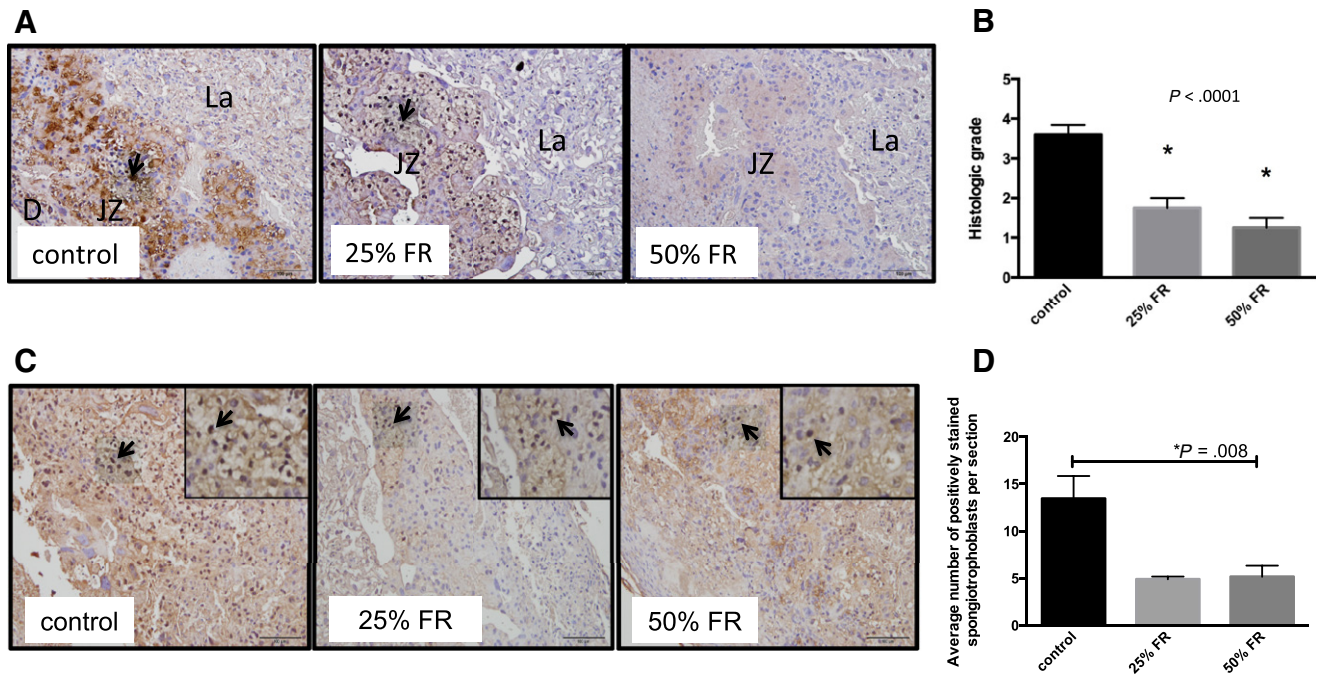
Fig. 5. – IL-10 and LC3B staining in murine placenta after maternal FR. A, Representative sections from each group (control, 25% FR, and 50% FR) stained for IL-10 demonstrate decreasing positive staining for IL-10 (brown; 20× magnification) with increasing severity of maternal FR. Arrows indicate positive staining. Scale bars represent 100 μm. D, decidua; JZ, junctional zone; La, labyrinth. B, Decreasing histologic grading scores of overall positivity of IL-10 staining in FR groups compared with controls (n = 4-7/group). Data are represented in graphs as means ± SEM. Asterisks indicate P < .0001 between the indicated group compared with the control group, by post hoc Tukey's multiple comparison testing. Listed P value represents significance between groups, by ANOVA. C, Representative sections from each group (control, 25% FR, and 50% FR) stained for LC3B (brown; 20× magnification) demonstrating decreasing numbers of positively stained spongiotrophoblasts in the junctional zone of FR mouse placenta with increasing severity of FR. Arrows indicate positive staining of spongiotrophoblasts. Scale bars represent 100 μm. D, Decreased average numbers of positively staining spongiotrophoblasts for LC3B per region of interest in FR groups compared with controls (n = 3 - 4/group). Data are represented in graphs as means ± SEM. Asterisk indicates P < .05 between all groups, by ANOVA.

human disease to also regulate autophagic and ER stress responses. In our model, we provide evidence that bulk measures of autophagy and ER stress are suppressed at the junctional zone of the murine placenta in conditions of maternal FR. These findings are contradictory to our hypothesis that IL-10 reduction leads to increased cellular death via autophagy and ER stress. Instead, these findings suggest that placental cell populations adapt to chronic nutrient restriction by decreasing cellular autophagic and ER stress responses to continue to function and survive to provide nutrients and blood flow to the growing fetus. We identified, by RNA sequencing and pathway analysis, novel genes important in these cell homeostasis regulatory pathways that are differentially affected by maternal FR. However, the suppression of autophagy, ER stress, and anti-inflammatory signals localized largely to the junctional zone in maternal FR-associated placentas does not adequately compensate for dysregulation of vascular and trophoblast structures within the murine labyrinth.

Autophagy is the process by which damaged organelles and protein aggregates are engulfed into autophagosomes, fused with lysosomes, and degraded by hydrolases. This process is essential for cell survival and regulation of energy

and nutrient homeostasis. Therefore, we had hypothesized that in our model of maternal FR and IUGR, markers of autophagy would be increased. However, we found the opposite—that bulk measures of autophagy are decreased. These contradictory findings are in line with the existing debate on whether placental insufficiency leads to induction or suppression of autophagy as some groups have shown that upregulation of autophagy is associated with fetal growth restriction and preeclampsia [24-26]. It is generally accepted that both in vivo and in vitro, starvation conditions activate autophagy. However, these responses are highly tissue specific, and modulated by multiple and complex input signals. The placenta is a unique organ that is responsible for sustenance of the growing fetus, often at the expense of maternal well being and, therefore, may regulate autophagic processes differently in response to nutrient deprivation.

Our results in placentas associated with FR overall suggest that bulk autophagy is decreased, especially in the junctional zone of the murine placenta. We believe that this seemingly contradictory finding may reflect the function of certain autophagy genes to inhibit inflammation, as seen in tissue-specific knock-out animal models of autophagy genes resulting in wide spread tissue over inflammation [27,28]. In
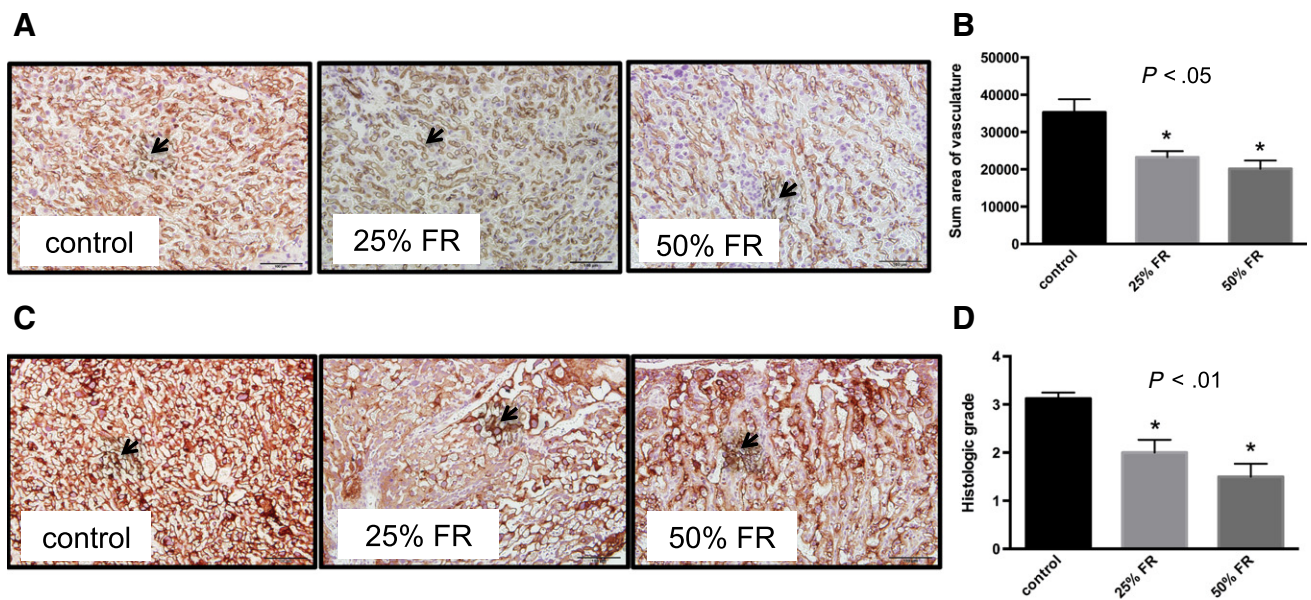
Fig. 6. – Vascular and trophoblast changes in the murine placenta with maternal FR. A, Representative sections from each group (control, 25% FR, and 50% FR) stained for CD34 (brown; 20× magnification) in endothelial cells within the labyrinthine region (20×). Arrows indicate blood vessels. Scale bars represent 100 μm. B, Quantitative analysis of sum of vascular area per region of interest at 40×. Each placental section from all 3 groups (n = 8/group) was analyzed in triplicate. Vascular areas were defined as outlined by contiguous positively stained cells. Data are represented in graphs as means ± SEM. Asterisks indicate P < .05 (between indicated FR group and control), by post hoc Tukey's multiple comparison testing. Listed P value indicates significance between all groups, by ANOVA. C, Representative placental sections from each group (control, 25% FR, and 50% FR) stained for trophoblast cells using cytokeratin (brown, 20× magnification). Qualitatively, degenerative changes (dilated maternal spaces, with a decreased percentage of positive stained cells in the 25% and 50% FR groups compared with controls) are seen in murine trophoblast layers within the labyrinth. Arrows indicate trophoblast lining. Scale bars represent 100 μm. D, Decreased histologic grading scores of overall positivity of cytokeratin stain in FR groups compared with controls (n = 8/group). Data are represented in graph as means ± SEM. Asterisks indicate P < .01 between indicated FR group vs control, by post hoc Tukey's multiple comparison testing. Listed P value indicates significance between all groups, by ANOVA.

fact, in in vivo cancer models, autophagy inhibition has been demonstrated to favor immunosuppression, leading to increased tumor aggressiveness [29]. If this is also true in pregnancy at the maternal-fetal interface, our results suggest that the autophagic suppression seen in the FR-associated placentas may represent a compensatory mechanism to maintain pregnancy in the face of a proinflammatory environment.

By RNA sequencing, we identified a number of autophagic genes that may be suppressed in IUGR induced by maternal FR. For example, Dram1, or DNA-damage regulated autophagy modulator 1, is a gene regulated as part of the p53 tumor suppressor pathway that encodes a lysosomal membrane protein required for the induction of autophagy via this pathway. In our murine FR-associated placentas, Dram1 expression was significantly decreased compared with controls implying suppressed autophagy via this pathway. This is in contrast to reports by Hung et al, who found increased levels of DRAM in human IUGR placentas [24]. Fbxo32, or F box protein 32 (also known as atrogin-1), deficiency in a knock-out animal model has been associated with premature death of cardiomyocytes via impaired autophagy [30]. In our model, FR led to decreased production of Fbxo32, perhaps affecting autophagy-induced cell death. Scd1, stearoyl-CoA desaturase 1, is a key player in fatty acid biosynthesis. Therefore, its

reduction in our FR groups may simply represent poor maternal nutrient supply. However, inhibition of Scd1 has been shown to reduce starvation-induced autophagy [31]. Therefore, the reduced levels of Scd1 seen in FR groups may reflect compensation in these placentas to reduce the induction of autophagy by starvation.

Endoplasmic reticulum stress is the disruption of protein folding in the ER, resulting in the accumulation of misfolded proteins within the ER. This pathologic process results from disturbances such as ER calcium depletion, nutrient deprivation, oxidative stress, DNA damage, or energy perturbation. When ER stress is persistent and excessive, the unfolded protein response initiates apoptosis to eliminate stressed cells and also activates nuclear factor–κB and the inflammasome. Endoplasmic reticulum stress has been implicated as a contributor to pathology in human IUGR, likely due to deficient placental perfusion inducing oxidative stress [32-35]. Again, our findings are contradictory to our hypothesis that ER stress increases in the nutritionally inadequate environment of IUGR. In our study, overall protein expression of BIP decreases with increasing severity of maternal FR, with no change in apoptotic markers between groups. This finding may again be related to the unique ability of the placenta to immunologically mediate stress responses

to maintain cellular viability and function to protect and provide for the developing fetus.

IL-10 has been found to modulate ER stress in other inflammatory disorders [36,37], but its role in placental ER stress has not been defined. By RNA sequencing, we have discovered 3 novel markers of ER stress that are differentially expressed in placentas of food-restricted mothers. We demonstrate decreased levels of Pdia4 (also known as ERP72), a mediator of the unfolded protein response, in FR groups compared with control mice. We also demonstrated decreased levels of Creld2, a stress-inducible gene that may regulate the ER stress response and progression. Mutations in promoter sites of this gene result in decreased basal activity and responsiveness to ER stress stimuli using luciferase reporter analyses [38]. Lastly, Derl3 was found to have decreased expression in FR placentas. Derl3 encodes an important component of ER-associated degradation. In vitro studies have demonstrated that overexpression of this gene enhances ER stress responses and promotes cellular survival, whereas decreased expression decreases ER response but increased cell death in response to ischemia [39]. Taken together, the decreased expression of these 3 genes would result in decreased functional ER stress activity in the face of nutritional deprivation.

Lastly, the protective effects of IL-10 on vascular function and inflammation have been observed both in pregnancy models and nonpregnancy states [22,23]. IL-10 knockout mice have been shown to exhibit impaired spiral artery remodeling and poor placental angiogenesis, resulting in IUGR, when exposed to environmental toxins. Treatment with recombinant IL-10 rescues the pregnancy, seemingly via restoration of endovascular activity [40]. Outside pregnancy, IL-10 has also been implicated as a mediator of vascular protection in hypertension, diabetes, and atherosclerosis [41-43]. Therefore, one interesting consequence of disordered IL-10 seen in adverse pregnancy outcomes is that it may be involved in vascular remodeling seen in placental insufficiency and the developmental programming of cardiovascular disease seen in the offspring of pregnancies complicated by IUGR, preeclampsia, or prematurity. An interesting candidate gene that was greatly increased in FR placentas is Map3k6 (mitogen-activated protein 3 kinase 6), which mediates angiogenic and tumorigenic effects via vascular endothelial growth factor expression [44]. Again, this increase may represent an attempt at compensation for poor placental vascularization secondary to nutritional restriction-induced remodeling, as is evident by our immunohistochemical staining for CD34+ endothelial cells. We also demonstrated decreased levels of C1qa, a polypeptide chain of complement subcomponent C1q. Complement C1q-induced activation of β-catenin signaling has recently been shown to contribute to hypertensive arterial remodeling [45]. Contrary to our expectations, C1qa levels were decreased in our FR placentas, again highlighting the inconsistencies of whether cellular protective mechanisms are impaired or enhanced in response to adverse environments in these pathologic conditions of pregnancy.

Our histopathologic findings were consistent with the reported placental findings in human IUGR [46,47], where placental hypovascularity and trophoblast degeneration lead to poor blood flow and nutrient transfer to the fetus [48].

However, it should be noted that despite decreased vascularity and damaged trophoblast layers within the labyrinthine area of FR-associated placentas, placental weight was not changed. It may be that in mild FR, placental mass is relatively maintained at the expense of fetal growth, whereas moderate FR crosses a critical threshold, beyond which placental self-preservation is impaired. Taken together, our histopathologic data suggest that alterations in immune tolerance and placental compensatory responses to protect cellular health via decreasing autophagic and ER stress responses, may allow for functional compensation at mild levels of FR, but are inadequate at more moderate levels of FR.

There are several strengths and limitations to our study. The use of animal models to study human disease is often necessary in diseases such as IUGR, where detection occurs late in the course of disease making progression of disease difficult to study. However, careful consideration into the specific animal model chosen is essential, as there are both similarities and differences to human placental structure and pregnancy with any animal model [49,50]. Though both mouse and human placentas are hemochorial, meaning fetally derived trophoblasts are directly bathed in maternal blood [48], there are significant differences in gestation and litter size, which may explain why human pregnancies demonstrate much greater adaptive capacity in protecting fetal weight. These differences present a major limitation of our study, as the extent to which animal data can be applied to human disease remains under debate. We specifically chose this mouse model of late chronic maternal FR as it has been shown to result in IUGR, and it has been well characterized in its effect of maternal health and hormonal status during pregnancy, nutrient transfer to the fetus, and short- and long-term effects on the offspring [7,48,51]. However, as stated previously, architectural differences in mouse and human placenta present challenges in comparing changes specific to the nutrient exchange layers. To address this, we used a discovery-based technique of RNA sequencing to identify patterns of placental gene expression changes that may be altered in growth restriction. This allows for a nonbiased evaluation of how specific genes involved in immunologic function and cellular maintenance are affected in IUGR, and identification of potentially novel players in placental insufficiency.

Using whole placenta, we found 700 genes that were significantly differentially expressed between groups, and performed pathway analysis, which demonstrated that the pathways of interest were well represented among the differentially expressed genes. However, another limitation of our study was that adjusted P values from RNA sequencing analysis were nonsignificant in some of our genes of interest involved in immunologic pathways. This limitation may have occurred because of the smaller sample sizes used for RNA sequencing. This sample size was chosen as genome-wide sequencing techniques applied to large groups can be cost prohibitive, and the main purpose of RNA sequencing in this study was to screen for pathway changes. To address this issue on a gene-specific basis, we validated RNA expression of specific genes of interest by qRT-PCR using larger sample sizes across all 3 experimental groups. In addition, there is still significant debate and remaining unknowns in the field

on the crosstalk between autophagy, ER stress and apoptotic pathways. Our study does not establish cause-and-effect, and further mechanistic studies on these pathways in IUGR are warranted to more definitively link decreased IL-10 with autophagy and ER stress.

In conclusion, our murine model of chronic, mild to moderate late gestational FR of the pregnant mouse represents an animal model of IUGR with reasonable fidelity to the human condition, based on histopathologic similarities. Consistent with our hypothesis, we found that IL-10 expression in the murine placenta is decreased in maternal gestational FR. Using RNA sequencing techniques, we have demonstrated that a significant portion of gene expression changes seen on a whole placental level involve immunologic pathways and associated cellular maintenance processes. However, contrary to our hypothesis that maternal FR results in increased autophagy and ER stress, leading to cellular death, we found that bulk measures of these pathways are decreased in maternal FR-associated placentas. We believe that these findings suggest that the placenta serves as a unique interface which must preserve fetal growth in the face of adverse maternal environment, and that these mechanisms are immunologically mediated. As such, placental compensatory responses appear to be distinct and opposite to the inflammatory, autophagic, and ER stresses described in in vitro nutrient deprivation.

Acknowledgment

REFERENCES

[1] Cross JC, Hemberger M, Lu Y, Nozaki T, Whitely K, Masutani M, et al. Trophoblast functions, angiogenesis and remodeling of the maternal vasculature in the placenta. Mol Cell Endocrinol 2002;187(1–2):207–12.

[2] Herr F, Baal N, Widmer-Teske R, McKinnon T, Zygmunt M. How to study placental vascular development? Theriogenology 2010;73(6):817–27.

[3] Kanaka-Gantenbein C. Fetal origins of adult diabetes. Ann N Y Acad Sci 2010;1205:99–105.

[4] Thornburg KL, O'Tierney PF, Louey S. Review: the placenta is a programming agent for cardiovascular disease. Placenta 2010;31:S54–9 [Suppl.].

[5] Ligi I, Grandvuillemin I, Andres V, Dignat-George F, Simeoni U. Low birth weight infants and the developmental programming of hypertension: a focus on vascular factors. Semin Perinatol 2010;34(3):188–92.

[6] Luyckx VA, Bertram JF, Brenner BM, Fall C, Hoy WE, Ozanne SE, et al. Effect of fetal and child health on kidney development and long-term risk of hypertension and kidney disease. Lancet 2013;382:273–83.

[7] Chen PY, Ganguly A, Rubbi L, Orozco LD, Morselli M, Ashraf D, et al. Intrauterine calorie restriction affects placental DNA methylation and gene expression. Physiol Genomics 2013; 45(14):565–76.

[8] Gabory A, Ferry L, Fajardy I, Jouneau L, Gothié JD, Vigé A, et al. Maternal diets trigger sex-specific divergent trajectories of gene expression and epigenetic systems in mouse placenta. PLoS One 2012;7(11):e47986.

[9] Mao J, Zhang X, Sieli PT, Falduto MT, Torres KE, Rosenfeld CS. Contrasting effects of different maternal diets on sexually dimorphic gene expression in the murine placenta. Proc Natl Acad Sci U S A 2010;107(12):5557–62.

[10] Biswas S. Placental changes in idiopathic intrauterine growth restriction. OA Anatomy 2013;1(2):11.

[11] Cheng SB, Sharma S. Interleukin-10: a pleitropic regulator in pregnancy. Am J Reprod Immunol 2015;73(6):487–500.

[12] Thamotharan S, Stout D, Shin BC, Devaskar SU. Temporal and spatial distribution of murine placental and brain GLUT3-luciferase transgene as a readout of in vivo transcription. Am J Physiol Endocrinol Metab 2013;304(3):E254–66.

[13] Trapnell C, Pachter L, Salzbery SL. TopHat: discovering splice junctions with RNA-Seq. Bioinformatics 2009;25:1105–11.

[14] Anders S, Huber W. Differential expression analysis for sequence count data. Genome Biol 2010;11(10):R106.

[15] Livak KJ, Schmittgen TD. Analysis of relative gene expression data using real-time quantitative PCR and the 2(–Delta Delta C(T)) method. Methods 2001;25(4):402–8.

[16] Ganguly A, McKnight RA, Raychaudhuri S, Shin BC, Ma Z, Moley K, et al. Glucose transporter isoform-3 mutations cause early pregnancy loss and fetal growth restriction. Am J Physiol Endocrinol Metab 2007;292(5):E1241–55.

[17] Sankar R, Thamotharan S, Shin D, Moley KH, Devaskar SU. Insulin-responsive glucose transporters-GLUT8 and GLUT4 are expressed in the developing mammalian brain. Brain Res Mol Brain Res 2002;107(2):157–65.

[18] Wadehra M, Natarajan S, Seligson DB, Williams CJ, Hummer AJ, Hedvat C, et al. Expression of epithelial membrane protein-2 is associated with endometrial adenocarcinoma of unfavorable outcome. Cancer 2006;107:90–8.

[19] Agley CC, Velloso CP, Lazarus NR, Harridge SD. An image analysis method for the precise selection and quantitation of fluorescently labeled cellular constituents: application to the measurement of human muscle cells in culture. J Histochem Cytochem 2012;60(6):428–38.

[20] Klopfleisch R. Multiparametric and semiquantitative scoring systems for the evaluation of mouse model histopathology—a systematic review. BMC Vet Res 2013;9: 123.

[21] Tinsley JH, South S, Chiasson VL, Mitchell BM. Interleukin-10 reduces inflammation, endothelial dysfunction, and blood pressure in hypertensive pregnant rats. Am J Physiol Regul Integr Comp Physiol 2010;298(3):R713–9.

[22] Chatterjee P, Chiasson VL, Kopriva SE, Young KJ, Chatterjee V, Jones KA, et al. Interleukin 10 deficiecy exacerbates toll-like receptor 3-induced preeclampsia-like symptoms in mice. Hypertension 2011;58(3):489–96.

[23] Chatterjee P, Chiasson VL, Seerangan G, Tobin RP, Kopriva SE, Newell-Rogers MK, et al. Cotreatment with interluekin 4 and interleukin 10 modulates immune cells and prevents hypertension in pregnant mice. Am J Hypertens 2015;28(1):135–42.

[24] Hung TH, Chen SF, Lo LM, Li MJ, Yeh YL, Hsieh TT. Increased autophagy in placentas of intrauterine growth-restricted pregnancies. PLoS One 2012;7(7):e40957.

[25] Oh SY, Choi SJ, Kim KH, Cho EY, Kim JH, Roh CR. Autophagy-related proteins, LC3 and Beclin-1, in placentas from pregnancies complicated by preeclampsia. Reprod Sci 2008;15(9): 912–20.

[26] Saito S, Nakashima A. A review of the mechanism for poor placentation in early-onset preeclampsia: the role of autophagy in trophoblast invasion and vascular remodeling. J Reprod Immunol 2014;101-102:80–8.

[27] Park S, Buck MD, Desai C, Zhang X, Loginicheva E, Martinez J, et al. Autophagy genes enhance murine gammaherpervirus

68 reactivation from latency by preventing virus-induced systemic inflammation. Cell Host Microbe 2016;19(1):91–101.

[28] Lu Q, Yokoyama CC, Williams JW, Baldrge MT, Jin X, DesRochers B, et al. Homeostatic control of innate lung inflammation by vici syndrome gene Epg5 and additional autophagy genes promotes influenza pathogenesis. Cell Host Microbe 2016;19(1):102–13.

[29] Ladoire S, Enot D, Senovilla L, Ghiringhelli F, Poirier-Colame V, Chaba K, et al. The presence of Lc3b puncta and hmgb 1 expression in malignant cells correlate with the immune infiltrate in breast cancer. Autophagy 2016 [epub ahead of print].

[30] Zaglia T, Milan G, Ruhs A, Franzoso M, Bertaggia E, Pianca N, et al. Atrogin-1 deficiency promotes cardiomyopathy and premature death via impaired autophagy. J Clin Invest 2014; 124(6):2410–24.

[31] Ogasawara Y, Itakura E, Kono N, Mizushima N, Arai H, Nara A, et al. Stearoyl-CoA desaturase 1 activity is required for autophagosome formation. J Biol Chem 2014;289(34): 23938–50.

[32] Burton GJ, Yung HW, Cindrova-Davies T, Charnock-Jones DS. Placental endoplasmic reticulum stress and oxidative stress in the pathophysioloy of unexplained intrauterine growth restriction and early onset preeclampsia. Placenta 2009; 30(Suppl. A):S43–8.

[33] Kawakami T, Yoshimi M, Kadota Y, Inoue M, Sato M, Suzuki S. Prolonged endoplasmic reticulum stress alters placental morphology and causes low birth weight. Toxicol Appl Pharmacol 2014;275(2):134–44.

[34] Lian IA, Løset M, Mundal SB, Fenstad MH, Johnson MP, Eide IP, et al. Increased endoplasmic reticulum stress in decidual tissues from pregnancies complicated by fetal growth restriction with and without pre-eclampsia. Placenta 2011;32(11):823–9.

[35] Yung HW, Calabrese S, Hynx D, Hemmings BA, Cetin I, Charnock-Jones DS, et al. Evidence of placental translation inhibition and endoplasmic reticulum stress in the etiology of human intra-uterine growth restriction. Am J Pathol 2008;173(2):451–62.

[36] Hasnain SZ, Tauro S, Das I, Tong H, Chen AC, Jeffery PL, et al. IL-10 promotes production of intestinal mucus by suppressing protein misfolding and endoplasmic reticulum stress in goblet cells. Gastroenterology 2013;144(2):357–68.

[37] Shkoda A, Ruiz PA, Daniel H, Kim SC, Rogler G, Sartor RB, et al. Interleukin-10 blocked endoplasmic reticulum stress in intestinal epithelial cells: impact on chronic inflammation. Gastroenterology 2007;132(1):190–207.

[38] Oh-hashi K, Koga H, Ikeda S, Shimada K, Hirata Y, Kiuchi K. CRELD2 is a novel endoplasmic reticulum stress-inducible gene. Biochem Biophys Res Commun 2009;387(3):504–10.

[39] Belmont PG, Chen WJ, San Pedro MN, Thuerauf DJ, Gellings Lowe N, Gude N, et al. Roles for endoplasmic reticulum-associated degradation and the novel endoplasmic reticulum stress response gene Derlin-3 in the ischemic heart. Circ Res 2010;106(2):307–16.

[40] Tewari N, Kalkunte S, Murray DW, Sharma S. The water channel aquaporin 1 is a novel molecular target of polychlorinated biphenyls for in utero anomalies. J Biol Chem 2009;284(22):15224–32.

[41] Gunnett CA, Heistad DD, Berg DJ, Faraci FM. IL-10 deficiency increases superoxide and endothelial dysfunction during inflammation. Am J Physiol Heart Circ Physiol 2000;279(4): H1555–62.

[42] Didion SP, Kinzenbaw DA, Schrader LI, Chu Y, Faraci FM. Endogenous interleukin-10 inhibits angiotensin II-induced vascular dysfunction. Hypertension 2009;54(3):619–24.

[43] Kinzenbaw DA, Chu Y, Peña Silva RA, Didion SP, Faraci FM. Interleukin-10 protects against aging-induced endothelial dysfunction. Physiol Rep 2013;1(6):e00149.

[44] Eto N, Miyagishi M, Inagi R, Fujita T, Nangaku M. Mitogen-activated protein 3 kinase 6 mediates angiogenic and tumorigenic effects via vascular endothelial growth factor expression. Am J Pathol 2009;174(4):1553–63.

[45] Sumida T, Naito AT, Nomura S, Nakagawa A, Higo T, Hasimoto A, et al. Complement C1q-induced activation of β-catenin signalling causes hypertensive arterial remodelling. Nat Commun 2015;6:6241.

[46] Biswas S, Adhikari A, Chattopadhyay JC, Ghosh SK. Histo-logical changes of placentas associated with intra-uterine growth restriction of fetuses: a case control study. Nepal Med Coll J 2012;14(1):18–24.

[47] Al-Sahan N, Grynspan D, von Dadelszen P, Gruslin A. Maternal floor infarction: management of an underrecognized pathology. J Obstet Gynaecol Res 2014;40(1): 293–6.

[48] Coan PM, Vaughan OR, Sekita Y, Finn SL, Burton GJ, Constancia M, et al. Adaptations in placental phenotype support fetal growth during undernutrition of pregnant mice. J Physiol 2010;588(Pt 3):527–38.

[49] Dilworth MR, Sibley CP. Review: transport across the placenta of mice and women. Placenta 2013(34 Suppl.):S34–9.

[50] Clark DA. The use and misuse of animal analog models of human pregnancy disorders. J Reprod Immunol 2014;103:1–8.

[51] Ganguly A, Collis L, Devaskar SU. Placental glucose and amino acid transport in calorie-restricted wild-type and Glut3 null heterozygous mice. Endocrinology 2012;153(8): 3995–4007.